A REVIEW AND INTERPRETATION OF RIA EXPERIMENTS

CARLO VITANZA
OECD-Nuclear Energy Agency, Le Seine Saint Germain, 12, boulevard des Îles
92130 Issy-les-Moulineaux, France
E-mail : Carlo.VITANZA@oecd.org

Received August 8, 2007

The results of Reactivity-Initiated Accidents (RIA) experiments have been analysed and the main variables affecting the fuel failure propensity identified. Fuel burn-up aggravates the mechanical loading of the cladding, while corrosion, or better the hydrogen absorbed in the cladding as a consequence of corrosion, may under some conditions make the cladding brittle and more susceptible to failure. Experiments point out that corrosion impairs the fuel resistance for RIA transient occurring at cold conditions, whereas there is no evidence of important embrittlement effects at hot conditions, unless the cladding was degraded by oxide spalling.

A fuel failure threshold correlation has been derived and compared with experimental data relevant for BWR and PWR fuel. The correlation can be applied to both cold and hot RIA transients, account taken for the lower ductility at cold conditions and for the different initial enthalpy. It can also be used for non-zero power transients, provided that a term accounting for the start-up power is incorporated. The proposed threshold is easy to use and reproduces the results obtained in the CABRI and NSRR tests in a rather satisfactory manner. The behaviour of advanced PWR alloys and of MOX fuel is discussed in light of the correlation predictions.

Finally, a probabilistic approach has been developed in order to account for the small scatter of the failure predictions. This approach completes the RIA failure assessment in that after determining a best estimate failure threshold, a failure probability is inferred based on the spreading of data around the calculated best estimate value.

KEYWORDS : RIA, High Burn-up, Corrosion, Cladding Brittleness, Failure Threshold

1. INTRODUCTION

Considerable experimental effort has been made in the last decade to produce experimental data in support of the definition of fuel safety limits at high burn-up. In particular, tests have been performed in specialised test reactors in order to characterize the fuel response to power transients representative of potential reactivity accidents postulated to occur in power reactors. The main objective of these tests was and is to assess the fuel failure limit (and possibly also the limit for fuel dispersal), as well as to provide the understanding needed to develop burn-up dependent safety criteria for RIA conditions. This paper concentrates on relatively recent data obtained with fuel specimens representative of the commercial fuel currently operating in nuclear power plants. Very old data and data obtained with fuel that had not been irradiated in power reactors but in test reactors, have not been included.

The main facilities where relevant RIA tests are being or have been generated recently are outlined below.

- The Japanese NSRR test reactor has produced a large amount of RIA fuel data at cold coolant conditions, i.e. approximately 20 ºC. This is an important detail since temperature affects the cladding brittleness, especially when a sufficient amount of hydrogen has been absorbed in the cladding as a consequence of corrosion during base operation. As summarized in Table 1 and 2, the NSRR tests have been made with both PWR and BWR fuel, mostly with Zr-4 and Zr-2 cladding, covering burn-up up to ~61MWd/kg and 79MWd/kg for BWR and PWR fuel respectively [1, 2, 3]. A limited number of tests have been conducted with MDA, NDA, ZIRLO and M5 alloy. The NSRR is by far the facility which has produced the largest amount of RIA test data for both PWR and BWR fuels, and the only source of new experimental results in recent years (2005-2007).
- The French CABRI reactor has focused on PWR fuel testing including MOX fuel. CABRI is the only source of modern RIA data obtained at hot coolant conditions, i.e. 280 ºC, which constitute a very valuable basis for the assessments of RIA starting at hot zero power conditions (HZP). Contrary to the NSRR, where RIA tests have been so far performed exclusively with short pulses (~5 ms), CABRI experiments have been carried out with different pulse width, typically in the range of 9-75 ms. The main parameters of these experiments are summarised in

Table 1. NSRR PWR Test Data (F=Fuel failure)

Rod N (PWR)	Bu MWd/kg	OX, μm	H, cal/g	D /1/	Calcul. H_F cal/g, /1/	Notes
MH1	39	4	47	1	180	
MH2	39	4	55	1	180	
MH3	39	4	67	1	180	
OK1	42	10	93	1	165	
OK2	42	10	90	1	165	
OI1	39	15	106	1	175	
OI2	39	15	108	1	175	
HBO1	51	43	**61 F**	0	69	
HBO2	50	35	37	0	75	
HBO3	50	23	74	1	134	
HBO4	50	19	50	1	135	
HBO5	44	60	**78 F**	0	79	
HBO6	49	33	85	0	79	
HBO7	49	45	88	0	73	
TK1	38	7	126	1	183	
TK2	48	35	**61 F**	0	72	
TK3	50	10	99	1	139	
TK4	50	15	98	1	137	
TK5	48	20	101	1	140	
TK6	38	15	125	1	179	
TK7	50	30	**86 F**	0	76	
TK8	50	10	65	1	139	
TK9	50	10	99	1	139	
TK10	46	10	86	1	151	
OI10	60	27	104	1	111	MDA
OI11	58	28	**120 F**	1	114	ZIRLO
OI12	61	41	143	1	106	NDA
VA1	78	73	**61 F**	0	51.1	MDA
VA2	79	70	**55 F**	0	51.8	ZIRLO
RH1	67	10	127	1	116	M5
MR1	71	39	89	1	107	NDA
BZ1	48	40	**74 F**	0	77	MOX
BZ2	59	20	**117 F**	1	112	MOX

Table 3 [4, 5]. The fuel had Zr-4 cladding in most cases, except three tests that were done with ZIRLO or M5 cladding. The oxide thickness ranged from 20 to 80mm, while the maximum burn-up was 77MWd/kg for UO_2 fuel and 62MWd/kg for MOX fuel.

Table 2. NSRR BWR Test Data (F=Fuel failure)

Rod N (PWR)	Bu MWd/kg	OX, μm	H, cal/g	D /1/	Calcul. H_F cal/g, /1/
TS1	26	6	55	1	200
TS2	26	6	66	1	200
TS3	26	6	88	1	200
TS4	26	6	89	1	200
TS5	26	6	98	1	200
FK1	45	16	130	1	151
FK2	45	18	70	1	150
FK3	41	24	145	1	162
FK4	56	22	140	1	120
FK5	56	22	70	1	120
FK6	61	25	**70 F**	0	61
FK7	61	25	**62 F**	0	61
FK8	61	25	65	0	61
FK9	61	25	**86 F**	0	61
FK10	61	25	**80 F**	0	61
FK12	61	25	**72 F**	0	61
LS1	60	25	**60 F**	0	62
DW1*	45	20	127	1	150

* MOX fuel in DW1

Table 3. CABRI Test Data (F=Fuel failure)

Rod N (PWR)	Bu MWd/kg	OX, μm	H, cal/g	Calcul. H_F cal/g, /1/	Notes
Na1	64	80	**30 F**	67	SP 9ms
Na2	33	4	199	200	9 ms
Na3	54	40	124	118	9 ms
Na4	62	80	85	115	75 ms
Na5	64	20	108	113	9 ms
Na6	47	35	133	144	MOX35ms
Na7	55	50	**114 F**	120	MOX40ms
Na8	60	130	**≤82 F**	66	SP 75ms
Na9	28	20	197	200	MOX 34ms
Na10	63	80	**81 F**	72	SP 31ms
Na11	63	15	93	119	31 ms
Na12	65	80	103	104	MOX 62ms
CIP01	75	79	90	100	ZIRLO32ms
CIP02	77	20	81	115	M5 28 ms

SP= Spalled cladding D=0 for spalled cladding
D=1 for all other cases

- The Russian IGR and BIGR reactors, which are the main source of RIA experimental data for VVER fuel [6, 7, 8]. The results are summarized in Table 4. The pulse width was very large in IGR (~700ms) and very short in BIGR (~3ms). Due to limitations in the test instrumentation, the enthalpy at failure could not be determined as it was done in the NSRR or CABRI tests. Thus, IGR and BIGR fuel failures data are reported in terms of maximum achieved fuel enthalpy (and not enthalpy at failure as for the NSRR and CABRI tests).

This paper focuses on PWR and BWR fuel, for which the NSRR and CABRI data are most relevant. The IGR and BIGR data are discussed here as they provide additional useful information, especially regarding failure predictions for cladding exhibiting low corrosion.

Table 4. IGR/BIGR Test Data (F=Fuel failure)

Rod N. (VVER)	Bu MWd/kg	Oxide +pulse width	H, cal/g	D /1/	Calculated H_F cal/g, /1/
H1T	49	≤5μm	151	1	162
H2T	48	in all	**<213 F**	1	165
H3T	49	tests	**<251 F**	1	162
H4T	49		114	1	162
H5T	49		**<176 F**	1	162
H6T	49	IGR,	87	1	162
H7T	47	700ms	**<187 F**	1	168
H8T	47	pulse	61	1	160
H14T	0		61	1	200
H15T	0		**<195 F**	1	200
H16T	0		121	1	200
H17T	0		91	1	200
H18T	0		85	1	200
H6C	0		**<219 F**	1	200
-------		--------			
RT1	48		142	1	146
RT2	48		115	1	146
RT3	48		138	1	146
RT4	60	BIGR,	125	1	117
RT5	49	3ms	146	1	145
RT6	48	puls	153	1	146
RT7	60		134	1	117
RT8	60		**<164 F**	1	117
RT9	60		**<165 F**	1	117
RT10	46		**<164 F**	1	150
RT11	49		**<188 F**	1	144
RT12	47		155	1	148

The NSRR and CABRI tests resulted in altogether 18 fuel failures out of 64 tests, i.e. 25-30% of the data are failures and 70-75% are non-failure events. It thus appears that a conservative approach where only the failure events are considered and where the failure threshold is merely defined by the lower envelope of the failure data, may not be fully satisfactory in that the largest portion of the experimental evidence, i.e. the non-failure data, would be disregarded.

The present paper provides a best-estimate RIA fuel failure correlation that takes into account all data, considering relevant parameters that can affect failure propensity and aiming to predict both failure and non-failure data, hence trying to discern differences among different data points in the best possible manner.

As discussed later, the proposed best-estimate threshold is satisfactory but, as one would expect, does not provide a perfect prediction of failures and non-failures in absolutely all cases. In fact, while data are generally predicted with good approximation, there are instances of failures and non-failures that are difficult to discriminate, possibly due to experimental uncertainties or because the cladding ductility may vary depending on conditions that are difficult to discern.

Because of the above, in addition to deriving a deterministic failure threshold, a probabilistic approach has been attempted here by defining a failure probability within an uncertainty band surrounding the best-estimate failure threshold value. The failure probability distribution within this band is defined on the basis of the whole data set, including both failures and non-failures, and accounting for the actual data scatter around the best estimate failure threshold.

In this manner, the entire experimental database is utilized to the maximum possible extent, firstly by extracting from it the knowledge needed to derive a best estimate failure threshold, and secondly by inferring from it a failure probability distribution around the best estimate threshold.

2. FUEL-CLADDING INTERACTION IN RIA

Pellet-cladding mechanical interaction (PCMI) is one of the fuel failure mechanisms associated with RIA testing. At increasing burn-up, PCMI-induced failures may occur at progressively lower fuel enthalpy as pointed out by the results shown in Fig. 1, where data from various RIA experiments are grouped in the same plot [3]. The figure indicates that failures at high burn-up can occur at much lower enthalpy than for low burn-up fuel.

The most important reasons for this behaviour are that:

- Fuel swelling and cladding creep-down result in a

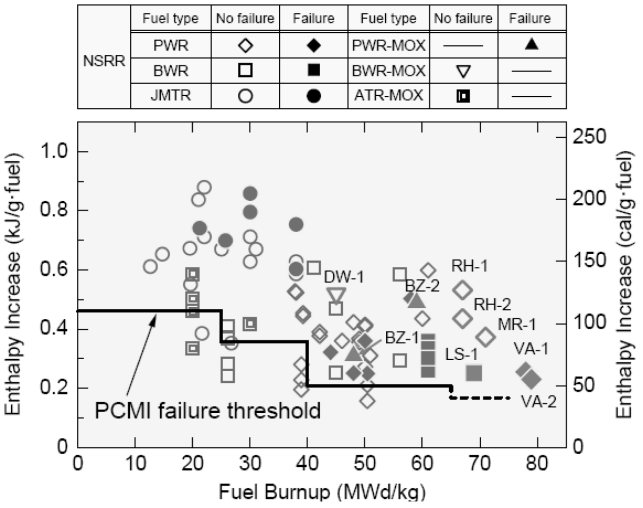

Fig. 1. Overall View of the NSRR Test Results, Showing a Pronounced Decrease of Failure Enthalpy with Burn-up [3]

progressive closure of the pellet-to-cladding gap during base irradiation. In RIA transients, this causes the PCMI to start at lower fuel enthalpy. The fact that high burn-up fuel is normally operated and conditioned at low power can also cause earlier PCMI onset. Further, the large fission product inventory at high burn-up can exacerbate the PCMI as the transient progresses.

- The cladding becomes more brittle with burn-up, partly due to irradiation but more importantly because of cladding corrosion and hydrogen pick-up. The cladding brittleness induced by the formation of hydride precipitates at the periphery of the cladding (hydride rim) is considered to be the major cause of the low enthalpy failures registered at high burn-up.

In other words, high burn-up induces an aggravation of the PCMI, while at the same time brittleness can reduce the cladding ability to withstand PCMI. This combination of factors can cause RIA failures to occur at relatively low enthalpy.

The experiments carried out in the NSRR and in the CABRI reactor show that low enthalpy failures, i.e. failures that occurred in the enthalpy range H_F<~85cal/g, were typically brittle failures. Starting from incipient cracks on the cladding outer surface, where the largest concentration of hydrogen is present, a crack may grow within the brittle portion of the cladding outer wall and eventually propagate through the cladding wall as a ductile fracture. An example of brittle failure is shown in Fig. 2 [3], which relates to a NSRR BWR fuel rod specimen (LS1, which failed at 60 cal/g). One can observe that the fracture, which started from the cladding OD, propagated in a brittle fashion up to ~60% of the cladding wall and continued thereafter as

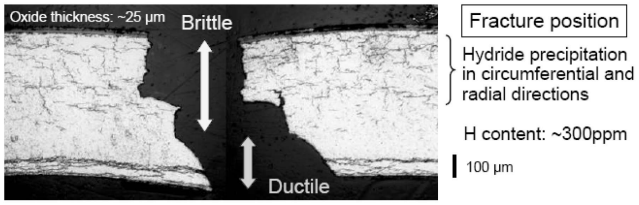

Fig. 2. View of the Through-wall Crack at the Failure Position in the LS-1 Test Fuel [3]

ductile fracture.

High burn-up fuel failures that occur in the range H_F>100cal/g normally entail appreciable cladding strain and are typically ductile failures. In this enthalpy range, additional burn-up phenomena become operative, contributing to cladding straining and possibly to fuel failure. The fuel microstructure undergoes significant changes linked to fission gas inventory and thus burn-up level. At the same time, the fission gas release also increases with enthalpy. Fuel swelling and fission gas release will add to each other contributing to increase the cladding strain. These mechanisms, in conjunction with the cladding heat-up causing a reduction of cladding strength, may eventually lead to failure.

In summary, the RIA failures can be broadly divided in two categories:

- Brittle failures, typically occurring in the low enthalpy range, i.e. 55-85 cal/g, which are basically caused by PCMI due to fuel thermal expansion. The driving force in this case is the *enthalpy change* during the RIA transient.
- Ductile failures, which are basically related to fuel and cladding heat up and to mechanisms consequent to such heat up. Ductile failures occurred at fuel enthalpy of ~115-120cal/g in the NSRR and CABRI experiments, and at ~150cal/g or higher in IGR and BIGR tests. Ductile failures are mainly determined by fuel and cladding heat up and should therefore be dependent on *fuel enthalpy level* (and not enthalpy increment as for brittle failures).

3. BRITTLE FAILURES

3.1 Experimental Basis

A plot of the failure enthalpy for the NSRR[1] and CABRI tests that resulted in fuel failure is given in Fig 3. As one can observe, all brittle failures are in the range of 55-85cal/g. One should also note that, since the enthalpy increment is the driving force for brittle failures, the two

[1] Excluding non-commercial test fuel

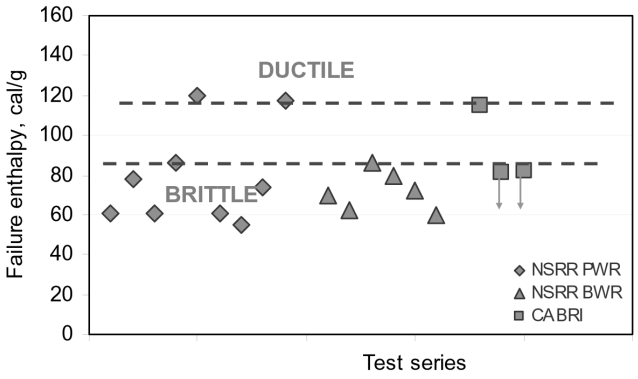

Fig.3. Range of Brittle and Ductile Failures in NSRR and CABRI Tests

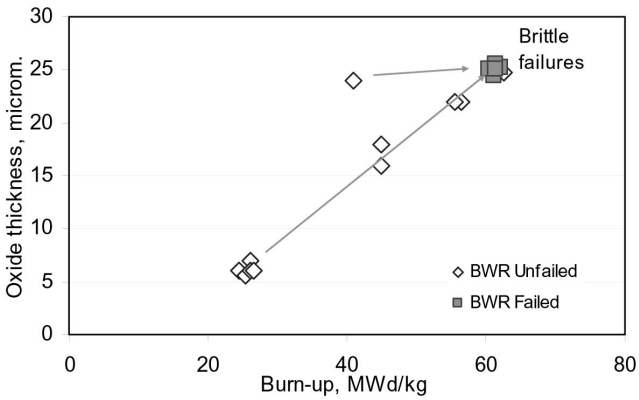

Fig.4. Corrosion Oxide Thickness vs. Burn-up for Non-failed and Failed NSRR BWR Fuel Rods

CABRI data points should be reduced by 18cal/g in order to be directly comparable with the NSRR data, thus accounting for the higher initial temperature conditions in CABRI as compared to NSRR (280 vs. 20ºC). This slight difference is pointed out by the two downward arrows in Fig.3.

The mean enthalpy increment at failure for the NSRR and CABRI brittle cases is ΔH_F=~70±15cal/g. The band of ±~15cal/g may be partly attributed to uncertainty of the experimental enthalpy determination. The differences in fuel power level in the last operating cycle, a parameter that is not further considered here, may also contribute to variations in failure enthalpy.

The NSRR tests with PWR fuel resulted in brittle failure in seven cases. For these, burn-up was in the range of 44-79 MWd/kg, while cladding corrosion was in the range 30-73 μm. Five of the seven PWR failures had Zr-4 cladding, whereas two had advanced cladding (ZIRLO and MDA). The ZIRLO and MDA failures, however, had very high burn-up and high corrosion, i.e. 78-79 MWd/kg and 70-73 μm.

BWR fuel failed in six NSRR tests. They were the BWR cases with the highest burn-up and highest corrosion, i.e. 60-61 MWd/kg and 25 μm. A distinct burn-up/ corrosion threshold appears to exist for the onset of brittleness in BWR cladding, as the diagram in Fig.4 clearly points out. As indicated in [3, 9], this is likely due to a larger hydrogen pick-up, possibly combined with an unfavourable hydride orientation in the Zr-2 cladding when burn-up approaches ~60MWd/kg. Whether this behaviour is induced by cladding hoop stress reversal due to fuel swelling or to other high burn-up phenomena, is a matter that remains to be clarified.

Fig.3 includes two CABRI brittle failures, which occurred for ΔH_F=63-64 cal/g. Both instances had high burn-up and large corrosion, i.e. 60-63 MWd/kg and 80-130 μm respectively. Other CABRI tests done with high burn-up and large corrosion fuel, however, did not result in fuel failure. As explained in [10], the distinct characteristics of the CABRI brittle failures is that they occurred only in the fuel rods that had oxide spalling during base irradiation, whereas, as already said, fuel that did not have spalling did not fail even if burn-up and corrosion were very high. A third CABRI test that had brittle failure, i.e. the debated Na-1 test[2], basically confirms that presence of spalling would cause brittle failure. The underlying mechanism is that spalling creates local cold spots on the cladding surface which function as centres for hydrogen accumulation, making the cladding very brittle and thus very vulnerable to PCMI failure.

The data discussed above indicate that the initial temperature may have a fundamental role in determining whether the fuel would fail at low enthalpy or not. At cold initial conditions such as in NSRR, low-enthalpy brittle failures can occur even for moderate corrosion (and appreciable burn-up). At hot initial conditions such as in CABRI tests, instead, brittle failures do not occur, or at least they did not occur in CABRI, even for high burn-up and high corrosion, unless oxide spalling was present. The distinction between cold and hot conditions is a key consideration for a correct interpretation of the experimental results and constitutes a relevant basis for the RIA failure correlation discussed in the remainder of this paper.

3.2 Brittleness at Cold Conditions

The NSRR results can be used to determine the effect

[2] The Na-1 test can be considered in qualitative terms, but, in the author's opinion, there are reasons to believe that the failure enthalpy might have been significantly higher than the currently reported value. Because of this, the Na-1 test is disregarded in the remainder of this paper.

of the corrosion-induced cladding brittleness for RIA transients occurring at cold zero power conditions (CZP). To this end, the Zr-2 and Zr-4 data have been plotted in Fig.5 in terms of enthalpy level vs. corrosion oxide thickness. One can observe that there are no brittle failures when the oxide thickness is <25 and 30μm for Zr-2 and Zr-4 respectively. Thus, as a conservative approximation, the oxide thickness of 25μm can be taken as the cold condition limit beyond which both Zr-2 and Zr-4 cladding becomes brittle.

A similar analysis of the NSRR data related to advanced (non Zr-4) PWR cladding suggest that such advanced alloys are able to withstand larger corrosion than Zr-4, before they become brittle. In fact, as Fig.6 shows, they (as a group) behave in a ductile manner for corrosion up to at least ~40-45μm, in spite of the burn-up being higher than 60 MWd/kg in most cases. Only the two instances with very high burn-up and very large corrosion resulted in brittleness and low-enthalpy failure. While these data need confirmation, the oxide thickness of 45μm can on a provisional basis be taken as the ductile - brittle transition limit for advanced PWR cladding at cold conditions.

It should be noted that the mechanisms leading to cladding brittleness are certainly more complex than a mere corrosion-induced transition, and that they are most probably linked to hydrogen pick-up and hydride orientation than to corrosion as such. However, a satisfactory description of the processes leading to increased hydrogen absorption and consequent cladding embrittlement in different types of cladding materials does not exist at present or at least is knot known to the author, which justifies the approximation made here to use corrosion thickness as an indicator of brittleness. Corrosion is, after all, the origin of hydrogen pick-up, and in addition oxide thickness is a directly measurable parameter, much more directly measurable than hydrogen content or hydride orientation.

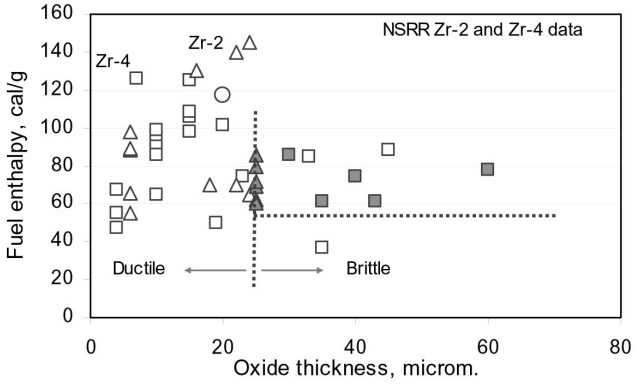

Fig.5. Fuel Enthalpy vs. Oxide Thickness for NSRR Tests with Zr-2 and Zr-4 Cladding. Brittle, Low Enthalpy Failures Appear to Occur for Oxide Thickness Larger than 25 μm

3.3 Brittleness at Hot Conditions

CABRI tests are the only one performed at hot initial conditions and are thus directly representative of RIA hot zero-power transients (HZP). As already mentioned, the main outcome of the CABRI tests run so far is that brittle failure does knot occur at hot coolant conditions, unless oxide spalling is present [10, 11].

Fig.7 reiterates this, showing a plot of all non-spalled CABRI data in terms of test enthalpy vs. oxide thickness. As one can observe, there is no indication of cladding brittleness, even for oxide thickness up ~80μm and burn-up in excess of 65MWd/kg. Failure of non-spalled fuel in

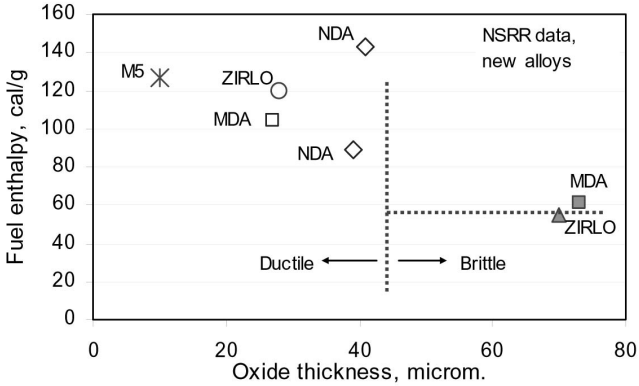

Fig.6. Fuel Enthalpy vs. Oxide Thickness for NSRR Tests with Advanced PWR Cladding. Brittle Fuel Failures Occurred Only for Large Oxide Thickness (Closed Symbols)

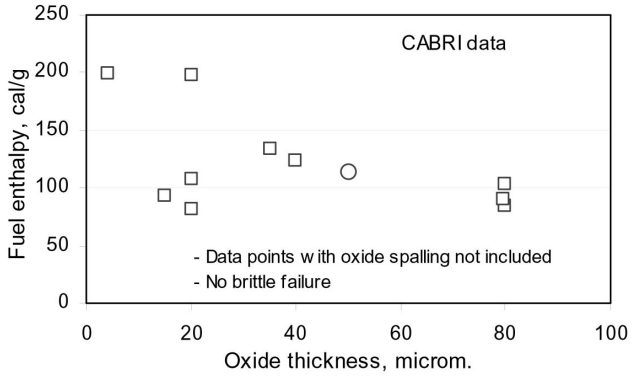

Fig.7. Fuel Enthalpy vs. Oxide Thickness for the CABRI Tests, Excluding the Data of the Tests with Oxide Spalling. No Brittle Failure was Observed, Even for Fuel Cladding with Large Corrosion. (The Circle Indicates the Na-7 Test).

CABRI occurred only in the Na-7 test, at 114cal/g. This, however, was a ductile failure, as post-irradiation examinations have shown [12].

One could argue that the ductile behaviour of (non-spalled) fuel in CABRI tests derives from the larger pulse width as compared with the NSRR tests. This is because larger pulses would to some extent allow cladding temperature to rise during the pulse itself, which would make the cladding more ductile as the PCMI develops. If this is true, it would reinforce the argument that starting a RIA at 280°C instead of 20°C should have a great impact on the cladding ductility and that the pulse effect, if relevant, would add to the initial temperature effect. Tests at hot coolant conditions as planned in NSRR, as well as future CABRI tests dedicated to the assessment of pulse width effects, will certainly help in clarifying this particular matter.

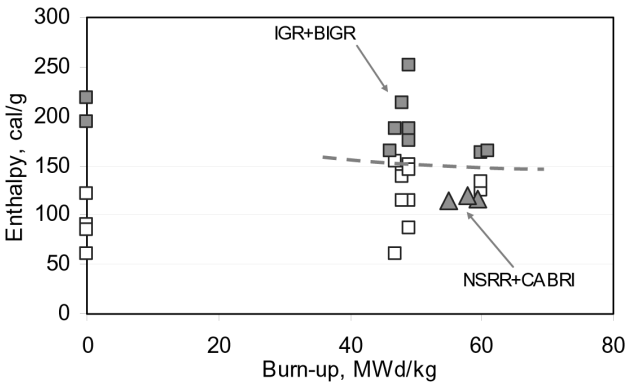

Fig.8. Onset of Failure for VVER fuel, as Compared with the NSRR and CABRI Ductile Failures

3.4. Conditions for Cladding Brittleness

The NSRR and CABRI test data can be summarised as follows:

- At cold conditions cladding is brittle if
  - Oxide thickness ≥25μm for Zr-2 and Zr-4 (Future tests may indicate whether burn-up affects this limit)
  - Oxide thickness ≥45μm for advanced PWR cladding[3]
- At hot conditions cladding is ductile, unless oxid spalling is present (and only then)
- Brittle failures are induced by PCMI and are determined by the enthalpy increment ΔH

4. DUCTILE FAILURES

As shown in Tables 1-3 and in Fig. 3, there are only three instances of ductile failures in the NSRR and CABRI database discussed here. Two failures occurred in NSRR PWR tests (OI-11 and BZ-2) and one in CABRI (Na-7). Of these, BZ-2 and Na-7 had MOX fuel and Zr-4 cladding, whereas OI-11 had UO_2 fuel and ZIRLO cladding. The burn-up was approximately the same in the three tests and ranged between 55 and 59MWd/kg. An interesting coincidence is that the failure enthalpy was very similar in the three tests, i.e. 117±3cal/g.

This enthalpy level corresponds to an average fuel temperature of ~1500-1600ºC, which is a range where phenomena linked to fission gas inventory become important. Temperature-induced overpressure of the fission gas stored at the grain boundary and grain boundary separation may cause pronounced fuel swelling, which adds to cladding loading due to fuel thermal expansion. Fission gas that may be released from the fuel matrix would also contribute to increase the cladding loading. The question as to whether fuel swelling or fission gas release is more important in determining the cladding loading in a RIA is a matter of debate and programmes are being put in place in order to ascertain it. However, the two phenomena are part of the same process, i.e. fuel overheating and grain boundary overpressure, and lead to the same consequence, i.e. additional cladding strain and eventually failure. An aggravating factor is the cladding temperature rise, which may cause a decrease in cladding strength and thus a reduction of fuel constraint. This may in turn have repercussion on the fission gas behaviour, which can be affected by the constraint level, especially for MOX fuel.

As the transient progresses towards higher enthalpy, i.e. well beyond 100cal/g, the fuel swelling and fission gas release on one side and the cladding heat-up on the other may at the end result in large cladding deformations and cladding burst, which appear to have been the cause for the fuel failure in the IGR and BIGR tests [8][4].

For the two failure mechanisms described here, i.e. cladding excessive strain due to swelling/fission gas release and cladding burst due to cladding heat-up and pressurisation, the driving parameter is temperature and thus enthalpy level. As shown in Fig.8, the failure enthalpy for these two mechanisms is, in the end, not so much different. In fact, the difference between the IGR/BIGR and the NSRR/CABRI enthalpy at failure onset is approximately ~30-35cal/g, which is appreciable but not very large. In reality, if one takes into account the fuel design difference between VVER and PWR/BWR fuel and in particular the

[3] These include MDA, NDA and ZIRLO. For M5, the only available data point is at very low corrosion.

[4] One should note that the cladding heat-up is expected to depend on the coolant conditions, and that none of the facilities addressed here had coolant conditions representatives for power reactor conditions. The NSRR, IGR and BIGR conditions, however, are expected to be conservative with respect to the mechanisms described above.

difference in cladding-to-fuel volume ratio, this difference becomes even smaller[5].

In summary, the mechanisms leading to ductile failures depend on the enthalpy level reached in the transient and failure occurrence can be expected when the fuel enthalpy exceeds ~100cal/g.

5. RIA FUEL FAILURE THRESHOLD

The following correlation, originally based on an analysis of CABRI post-test strain data [13], has been derived to determine the RIA fuel failure threshold

$$H_F=\left[200\cdot\frac{25+10D}{Bu}+0.3\Delta\tau\right]\left(1-\frac{0.85OX}{W}\right)^2-\delta H \qquad (1)$$

Where:
- D=0 (brittle) for cold conditions when
  - OX≥25μm for Zr-2 and Zr-4 or
  - OX≥45μm for advanced PWR cladding
- D=1 (ductile) for remaining cold conditions and for hot conditions unless spalled (if so, D=0).
- H_F is failure enthalpy, cal/g. If H_F>200, set H_F=200
- δH =18cal/g for CZP and brittle case, otherwise δH=0
- $\Delta\tau$ is pulse width, ms. If $\Delta\tau$>75ms, set $\Delta\tau$=75
- W is cladding thickness, as-fabricated, μm
- OX is oxide thickness, μm
- Bu is burn-up, MWd/kg. If Bu>60 set Bu=60

The main characteristics of the above correlation are described below.

Burn-up effect: Data at low and intermediate burn-up show an enhancement of strain with burn-up up to ~50-60MWd/kg mainly due to gap closure [14]. This is the reason for the pronounced burn-up effect acknowledged in Eq.(1). Data in the very high burn-up range show no evidence of additional cladding strain enhancement as burn-up progresses beyond 55-60MWd/kg [14]. This is why the burn-up effect in Eq(1) is limited up to 60 MWd/kg. Burn-up affects the predicted failure threshold directly (through the term Bu) and indirectly trough the oxide thickness (OX) and ductility term (D).

Fig.9 shows the predicted failure enthalpy vs. burn-up for PWR fuels with high and low (advanced cladding)

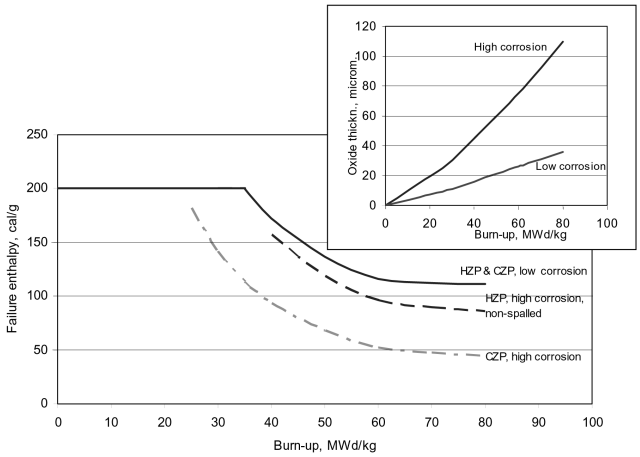

Fig.9. Calculated Failure Enthalpy vs. Burn-up for Two PWR Instances, Respectively with High and Low Corrosion, the Latter for Advanced Cladding. The Corrosion Build-up for the Two Instances is Given in the Upper-right Diagram. The Predicted Corrosion Effect is Very Large for CZP Conditions and Moderate for HZP (with Non-Spalled Fuel Cladding).

corrosion. As one can observe, corrosion has a much more pronounced effect for a CZP than for a HZP RIA. This is because corrosion induces cladding brittleness at cold conditions, which is not predicted to happen at hot conditions, unless oxide spalling is present.

Corrosion effect: The corrosion effect is accounted for in Eq.(1) by means of the term OX and, more importantly, by the ductility term D. An example of the quality of the predictions is given in Fig.10, which gives a comparison of the measured and calculated failure enthalpy are for the NSRR PWR tests that resulted in fuel failure. As one can notice, the predictions are very satisfactory. It should be pointed out, in this context, that

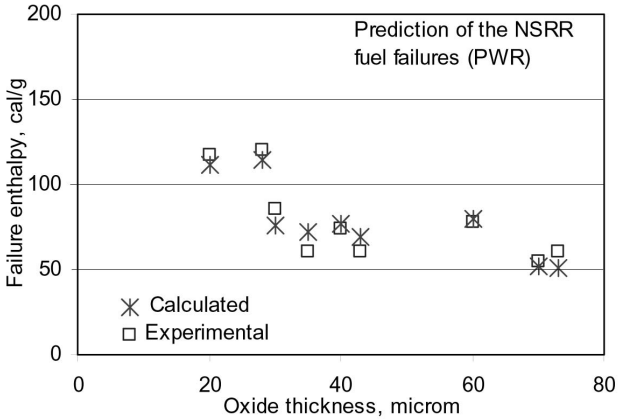

Fig.10. Calculated and Measured Failure Enthalpy vs. Oxide Thickness for NSRR Tests with PWR Fuel

[5] The fuel-to-cladding ratio is larger in BWR/PWR than in VVER. Considering this design difference and the mechanisms involved, which are basically linked to fuel and cladding heat-up, the IGR/BIGR data should be reduced by roughly 10% in order to be more directly comparable with the NSRR/CABRI data. This would bring the IGR/BIGR and the NSRR/CABRI (ductile) failure level even closer than shown in Fig.8.

while Eq.(1), predicts a significant impact of corrosion for CZP conditions, the corrosion effect at hot conditions is predicted to be much less pronounced (for non-spalled cladding). One should also add that corrosion and burn-up act in synergy with each other, in that the burn-up effect becomes stronger when the corrosion is high and corrosion effects become more important when burn-up is high. Thus, expressing the RIA failure limit only in terms of burn-up or only in terms of corrosion oxide thickness represents, in the author's opinion, an oversimplification.

Pulse width effect: The present fuel failure correlation acknowledges only a moderate pulse width effect, in that a change in pulse width from for instance 5 to 70 ms would result in a 20cal/g increment in fuel failure threshold. The basis for such moderate effect lays in the available experimental data, which do not point out any evident pulse width effect. Future experiments may enlighten this matter. In planning them, preference should go for test fuel having appreciable corrosion and high burn-up, since pulse width is expected to be insignificant for ductile cladding, as the IGR and BIGR tests have demonstrated[6].

Cold vs. hot initial conditions: The present correlation attributes great importance to whether the test starts at cold or hot conditions. This is because temperature affects ductility, which in turn affects the failure enthalpy (through the parameter D). Another less important factor is the term δH, which accounts for the lower initial enthalpy for the CZP brittle transients, which depend on enthalpy increment ΔH (whereas ductile transients depend on enthalpy level). The effect of cold vs. hot coolant conditions on failure threshold predictions is evidenced in Fig.9.

Behaviour of PWR advanced cladding: The greatest benefit of advanced PWR cladding alloys is represented by their capability to limit corrosion, hence avoid brittleness. Their importance is expected to be grater for CZP transients, for which brittleness is an issue, than for hot transients, for which cladding can retain ductility regardless of corrosion unless it was spalled. The CZP data so far available indicate that in order to be effective, advanced alloys should not oxidise beyond a certain limit, provisionally set at 45μm. If corrosion becomes excessive the advantage would disappear, as the VA-1 and VA-2 tests have pointed out. More data, however, are needed to confirm the improvements that are anticipated for advanced cladding.

Behaviour of MOX fuel: The experimental and calculated failure threshold vs. burn-up for all NSRR and CABRI MOX fuel are plotted in Fig.11. As one can observe, the quality of the predictions is very good. The predictions follow the data very closely, including the BZ-1 failure, which occurred at appreciably lower enthalpy than the other tests. The low failure enthalpy in this instance is due to the combined effect of corrosion level and cold test conditions. There were three MOX failures out of seven tests, corresponding to a failure rate of ~45%, which is much higher than for UO_2 fuel (~25%). However, as Fig.11 shows, the MOX fuel was pushed to a relatively high enthalpy level in all tests[7], i.e. very close or above the expected failure threshold, which was not the case for the UO_2 tests. The present evaluation shows that the failures of MOX fuel can be well predicted by the same failure threshold correlation used for UO_2 fuel, leading to the conclusion that a different treatment of MOX fuel as compared with UO_2 fuel is not needed, at least for what concerns failure threshold. Nevertheless, this does not exclude that other aspects could be different, for instance in relation to the post-failure behaviour of the two types of fuel.

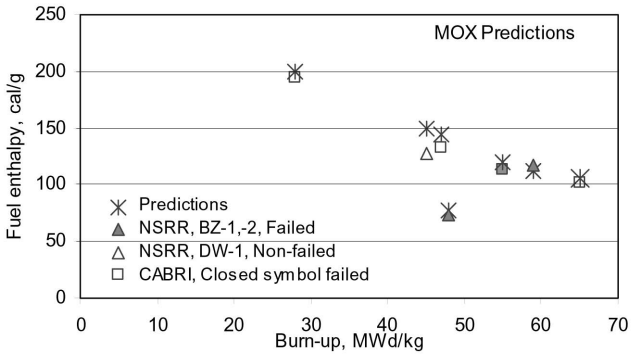

Fig.11. Calculated Failure Enthalpy and Measured Enthalpy for the MOX Fuel Tests Performed in NSRR and CABRI

Non-zero power RIA: As discussed in [14] the failure threshold can be applied also for a RIA starting at a certain power. In this case the failure threshold will be obtained by subtracting the term (1.4·LHR) from the failure enthalpy calculated by Eq.(1), where LHR (KW/m) is the heat rating at transient start.

Correlation capability: The overall predictive capability of the correlation discussed above is shown in Fig.12, where the predicted failure enthalpy is plotted

[6] The cladding for the future tests envisaged here should have no spalling, as CABRI tests have already shown that spalled cladding would fail for any pulse width.

[7] With the exception of the DW-1 test, which reached 127 cal/g while the predicted failure enthalpy is 150 cal/g

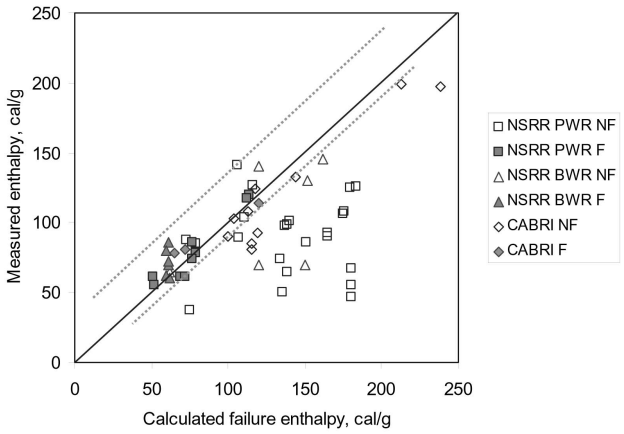

Fig.12. Calculated vs. Measured Enthalpy. Predictions are Satisfactory in that ~ 85% of the Non-failed Test Data are Below the Median Line and ~ 85% of the Failed Cases are Along or Above the Median Line. The Two Dotted Lines Parallel to the Median Line Correspond to 0% and 100% Failure Probability, Where the Latter is Calculated with Eq.2.

against the measure value for all the NSRR and CABRI data discussed here. The predicted failure threshold for the NSRR, CABRI and IGR/BIGR tests is also reported in Table 1 to 4.

In general, the predictions appear to be rather satisfactory in that:

- Failure and non-failure data are well separated and correctly predicted in ~85% of the cases. That is, 85% of the non-failed data points are below the median line which means correct prediction, and 85% of the failed data points lay at or are above the median line – which means correct or slightly conservative prediction.
- In only three cases the predictions were non-conservative in that the measured failure enthalpy was noticeably lower than the predicted value. However, the difference is rather small, i.e. 11cal/g or less.

One can then conclude that the present correlation is able to discriminate failures and non failures in a satisfactory manner. There remains however some imperfection in that some few data points are "on the wrong side" of the median line, in that some data are above and few failed data are below it. These imperfections can be accounted for by means of a statistical approach, as described in the next section.

6. PROBABILISTIC APPROACH

While the median line in Fig.12 corresponds to the deterministic best-estimate failure threshold expressed by Eq.(1), a failure probability can be defined as a function of the distance from the best estimate threshold, i.e. for any line parallel to the median line in Fig.12. As this line is moved upwards, the probability of failure will increase, reaching 100% at the upper envelope of all experimental data.

The failure probability vs. distance from the best estimate threshold is calculated as follows:

$$P=N_{F\leq}/\,[N_{F\leq}+N_{>}] \qquad (2)$$

where $N_{F\leq}$ is the number of failure events that occurred below or along a given line parallel to the median line of Fig.12 and $N_{>}$ are the events (failed and non-failed) above such line. The zero probability corresponds to the lowest failed data point, while 100% probability corresponds to the uppermost data point, as indicated by the dotted lines in Fig.12.

The failure probability as a function of distance from the best estimate failure threshold is shown in Fig.13. One can note that:

- The failure probability starts increasing when enthalpy is 15cal/g below the best estimate threshold. As an example, if the best estimate failure enthalpy was, say, H_F =80cal/g, the failure probability would be P=0 for enthalpy H≤65cal/g.
- The failure probability is 10% when enthalpy is 5cal/g below the calculated threshold, 17% for enthalpy equal to the threshold and 50% when enthalpy is 8cal/g above the threshold. For the example of a calculated threshold H_F = 80cal/g, this would mean a 50% failure probability for enthalpy H=88cal/g.

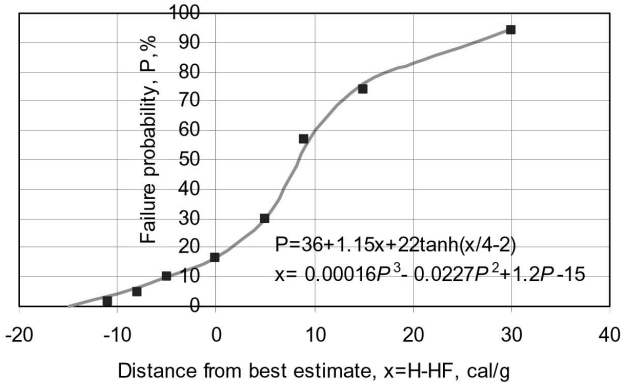

Fig.13. Failure Probability vs. Distance from the Best Estimate Failure Threshold, Derived by Means of Eq./2/ from the Data Distribution Shown in Fig.12

The mathematical expression of the failure probability *P*, in %, as function of distance from best

estimate threshold, $x=H-H_F$, in cal/g, is as follows:

$$P=36+1.15x+22\tanh(x/4-2) \quad (3)$$

The inverse of this equation is expressed by the following polynomial fit:

$$x= 0.00016P^3- 0.0227P^2+1.2P-15 \quad (3')$$

or equivalently:

$$H=H_F + 0.00016P^3- 0.0227P^2+1.2P-15 \quad (3'')$$

In the latter H is the enthalpy associated to a given failure probability P, H_F being the best estimate failure threshold calculated by means of Eq.(1)

The probabilistic approach described here completes the RIA failure assessment in that it utilises the data to the maximum possible extent, firstly by inferring a best estimate failure threshold which discriminates failures and non-failures in the best possible way, and secondly by inferring a failure probability based on the spreading of data around the best estimate failure threshold.

For what concerns its possible utilisations, failure probability can in principle be used to estimate a test outcome in advance of its execution. On a broader basis, it could also be used to provide estimates of the expected core damage, in conjunction with calculated core enthalpy distributions. Additional aspects, such as the uncertainty associated with enthalpy calculations, are also of interest in this context, but go beyond the intent of this paper.

7. CONCLUSIONS

– NSRR and CABRI experiments have provided a very valuable database for PWR and BWR fuel behaviour in a RIA transient. Cladding corrosion is a limiting factor at cold initial conditions, whereas there are no apparent embrittlement effects at hot conditions for fuel that has no oxide spalling. Spalling degrades significantly the fuel performan-ce and was the cause of the three brittle failures that were observed in CABRI.
– Future NSRR tests run at hot conditions are expected to clarify the effect of the initial coolant temperature on the fuel capability to survive a RIA.
– There is no evidence that MOX fuel behaves differently that UO_2 in terms of failure propensity.
– Tests with advanced PWR cladding seem to indicate an improved performance with respect to Z-4, but the database is still scarce and needs to be extended.
– An easy to use correlation has been proposed in order to calculate the fuel failure limit depending on burn-up, extent of cladding oxidation and coolant initial conditions
– The proposed correlation predicts failures and non-failure events in a rather satisfactory manner.
– In addition, a correlation has been derived in order to calculate the failure probability vs. enthalpy for given coolant initial conditions and fuel characteristics.

ACKNOWLEDGEMENT

This paper reflects the author's interpretation of the work of many experimentalists, who are collectively thanked for their important contributions to fuel knowledge.

REFERENCES

[1] T. Fuketa, *"JAERI Experimental Basis on RIA and LOCA"*, presentation made at the CSNI/CNRA meeting, December 2004.
[2] T. Fuketa, *"Fuels Safety Research at JAEA"*, 2007 Fuel Safety Research Meeting, Tokai-mura, Japan, May 2007.
[3] T. Sugiyama, *"PCMI Failure of High Burn-up Fuels under RIA Conditions"*, 2007 Fuel Safety Research Meeting, Tokai-mura, Japan, May 2007.
[4] J. Papin, *"Synthesis of the CABRI Programme Interpretation"*, Eurosafe meeting, Paris, November 2003.
[5] J. Papin, *"IRSN Experimental Basis for High Burn-up Fuel"*, presentation made at the CSNI/CNRA meeting, December 2004.
[6] V. Asmolov, L. Yegorova, *"Development and Performance of Research Programme for Analysis of High Burn-up Fuel Rod Behaviour Under RIA Conditions at IGR Pulse Reactor"*, OECD Specialist Meeting on Transient Behaviour of High Burn-up Fuel, NEA/ CSNI/R(95)22, Cadarache, France, Sept. 1995
[7] G. Abyshov et al., *"Data Base on the Behaviour of High Burn-up Fuel Rods with Zr-1%Nb Cladding and UO_2 Fuel (VVER Type) under Reactivity Initiated Accident Conditions"*, NUREG/IA-0156, July 1999.
[8] Y. Bibilashvili *et al., "Study of High Burn-up VVER Fuel Rod Behaviour at the BIGR Reactor under RIA Conditions: Experimental Results", OECD Topical Meeting on RIA Fuel Safety Criteria,* NEA/CSNI/R(2003)8, Vol.2, Aix-en-Provence, France, May 2002.
[9] P. Clifford, J. Voglewede, *"A Regulatory View of Reactivity -Initiated Accident Criteria in the U.S."*, 2007 Fuel Safety Research Meeting, Tokai-mura, Japan, May 2007.
[10] J.M. Conde Lopez, *Joint statement regarding the interpretation of the UO_2 REP-Na tests except REP- Na-1*, March 2007.
[11] C. Vitanza, *"RIA Failure Threshold and LOCA Limit at High Burn-up"*, Journal of Nuclear Science and Technology, Atomic Energy Society of Japan, vol.43, September 2006.
[12] B. Cazalis, *"Status of the Interpretation of the MOX CABRI REP-Na Tests"*, CABRI Review Meeting, June 1999.
[13] C. Vitanza and J.M. Conde Lopez, *"PCMI Implications for High Burn-up Light-Water Reactor Fuel in Reactivity*

Initiated Accidents", Seminar on Pellet-Clad Interaction in Water Reactor Fuels (PCI-2004) Aix-en-Provence, 9-11 March 2004, OECD 2005, ISBN 92-64 01157-9.

[14] C. Vitanza, *"Considerations on Burn-up Dependent RIA and LOCA Criteria", 2005 Water Reactor Fuel Performance Meeting, Kyoto, Japan*, October 2005.